Pergamon

Int. J. Heat Mass Transfer. Vol. 41, No. 17, pp. 2697–2704, 1998

Printed in Great Britain
0017–9310/98 $19.00+0.00

PII: S0017–9310(97)00110–5

The radiation transfer in emitting, absorbing and scattering media of complex geometric form

O. G. MARTYNENKO, M. L. GERMAN, V. P. NEKRASOV and E. F. NOGOTOV
Heat and Mass Transfer Institute, Belarus Academy of Sciences 15 P Brovka, Minsk, 220728, Belarus

(*Received* 2 *December* 1996)

Abstract—A numerical algorithm for radiative transfer characteristics calculation in an absorbing, scattering and emitting medium of various multidimensional geometry is proposed. Some results of numerical investigation of the influence of optical properties and geometric form of medium on the radiative transfer characteristics are discussed.

1. INTRODUCTION

The study of the mechanism of radiation propagation has a great significance for different scientific branches. They include radiative and complex heat transfer, spectroscopic analysis of plasma, structure and thermal conditions of planetary atmospheres and others. An analysis of the literature shows that this problem is being elaborated by the researchers in different scientific centers. As a result, at present there are a lot of methods for the numerical solution of the radiative transfer problem in the participating media. These are such methods as the Monte-Carlo method [1], zone method [2], spherical-harmonics approximation [3], radiation element method [4], method of characteristics [5], discrete ordinates method [6–9] and others. Each of them has its own advantages and disadvantages. At this point it should be noted that, while investigating the radiative transfer in selectively absorbing, emitting and scattering media of complex geometry, none of those methods can provide a high accuracy of computation when the computer resources have reasonable limits. That is why a solution algorithm free of marked demerit and some results of numerical investigations of the influence of geometric form and optical properties of medium on the radiative transfer characteristics under the conditions which are typical for furnaces in power plants are proposed in the paper.

2. METHOD

2.1 *Mathematical model*

The equation describing the transfer of monochromatic radiation under the condition of local thermodynamic equilibrium in an absorbing, scattering and emitting medium has the following form:

$$\bar{l}\cdot\nabla I(\bar{r},\bar{l})+(\chi(\bar{r})+\sigma(\bar{r}))I(\bar{r},\bar{l}) = \chi(\bar{r})B(T(\bar{r}))+\frac{\sigma(\bar{r})}{4\pi}\int_{4\pi}p(\bar{r},\bar{l},\bar{l}')I(\bar{r},\bar{l}')\,\mathrm{d}\Omega'. \quad (1)$$

Boundary conditions for radiative transfer equation (1) for media bounded by a surface of favorable curvature are of the form [5]:

$$I(P,\bar{l})|_{(\bar{l}\cdot\bar{n})<0} = I_0(P,\bar{l}) + \frac{1}{\pi}\int_{2\rho}\pi(P,\bar{l},\bar{l}')\cdot I(P,\bar{l}')\cdot(\bar{l}'\cdot\bar{n})\,\mathrm{d}\Omega' \quad (2)$$

where $\rho(P,\bar{l},\bar{l}')$ is a reflection distribution function of a bounding surface; $I_0(P,\bar{l})$ is an incident radiation intensity at the boundary point P. This condition (2) may be written for model surfaces as follows:

(1) diffuse–emissive surface

$$I(P,\bar{l})|_{(\bar{l}\cdot\bar{n})<0} = \varepsilon(P)B(T_W)+\frac{1-\varepsilon(P)}{\pi}Q_p \quad (3)$$

where

$$Q_p = \int_{(2\pi)} I(P,\bar{l}')\cdot(\bar{l}',\bar{n})\cdot\mathrm{d}\Omega'$$

(2) specular surface

$$I(P,\bar{l})|_{(\bar{l}\cdot\bar{n})<0} = I(P,\bar{l}') \quad (4)$$

where $\bar{l}'$ is a direction of ray which has been reflected on the surface to the direction $\bar{l}$;

(3) transparent surface

$$I(P,\bar{l})|_{(\bar{l}\cdot\bar{n})<0} = I_0(P,\bar{l}) \quad (5)$$

where $I_0(\mathrm{P},\bar{\mathrm{l}})$ is the radiative intensity which is incident to the participation medium.

The scattering phase function is usually determined through the Legendre's polynomials as [6, 7]

NOMENCLATURE

$I(\bar{r}, \bar{l})$	intensity of radiation at the point $\bar{r}$ along direction of propagation $\bar{l}$	Sc	albedo for scatter
$\chi(\bar{r})$, $\sigma(\bar{r})$	absorption and scattering coefficients	ε	emissivity of a boundary surface
$B(T)$	Plank's blackbody radiation at the temperature T	$\bar{n}$	external normal to a bounding surface
$p(\bar{r}, \bar{l}, \bar{l}')$	radiation scattering phase function	W	considered volume
Q_p	density of outgoing radiant flux on the boundary surface	Ω	solid angle
τ	optical density of medium	T_w	temperature of boundary surface
		T_b	temperature of medium near the boundary surface
		$q = Q/Q_{max}$	reduced density of outgoing radiant flux on the boundary surface.

$$p(\bar{r}, \bar{l}, \bar{l}') = \sum_{n=0}^{N} (2n+1) \cdot a_n \cdot P_n(\bar{r}, \bar{l} \cdot \bar{l}'). \quad (6)$$

As is shown in ref. [10], for many cases the phase function may be determined in the 'transport' approximation:

$$p(\bar{r}, \bar{l}, \bar{l}') = a(\bar{r}) \cdot [1 + 4\pi\delta(\bar{l} \to \bar{l}')] \quad (7)$$

where $a(\bar{r})$ is a double part of downward radiation scattering on its interaction with an elementary volume of medium. In this case, equation (1) with anisotropic scattering is transformed to an equation with isotropic scattering by the substitution of σ on $a \cdot \sigma$.

2.2. *Numerical method*

The solution algorithm of the integro-differential equation (1) with boundary conditions (2) is a combination of the discrete–ordinate method [1, 5], and the finite element method [11]. According to the discrete–ordinate method, the radiative propagation directions ($N_d = 2 + N_\phi \cdot N_\theta$) are given. Here, N_ϕ is the directions number over the polar angle ($0 \leqslant \phi \leqslant 2\pi$) and N_θ is the directions number on the azimuthal angle ($0 \leqslant \theta \leqslant \pi$). For each direction, $k = 1, \ldots, N_d$, equation (1) is represented as

$$\bar{l}_k \cdot \nabla I(\bar{r}, \bar{l}_k) + \alpha(\bar{r}) \cdot I(\bar{r}, l_k) = S^k(\bar{r}) \quad (8)$$

where S^k is the so-called source function along the direction, $\bar{l}_k$, which is determined by the right-handside of the equation (1), $\alpha = \chi + \sigma$ is the extinction coefficient and $\bar{l}_k = \sin\theta_k \cdot \cos\phi_k \cdot \bar{i} + \sin\theta_k \cdot \sin\phi_k \cdot j + \cos\theta_k \cdot \bar{k}$.

According to the finite element method, the discretization of the calculative domain into finite elements is made. As a result of this procedure we receive a number of elements (N_e) and nodes or grid points (N_p), for which the value of radiative intensity has to be computed in every direction.

The linear basis function $\psi_i(\bar{r})$ is selected for a typical grid point, $i = 1, \ldots, N_p$. This function satisfies the conditions $\psi_i(\bar{r}_i) = 1$ and $\psi_i(\bar{r}_j) = 0$ for every $j \neq i$. Then, the radiant intensity for the kth direction may be formulated through basis functions:

$$I^k(x, y, z) = \sum_{i=1}^{N_p} I_i^k \cdot \psi_i(x, y, z) \quad (9)$$

where I_i^k is the radiative intensity in the ith node along the kth direction. Using the Galerkin method [8, 11] the finite element form of the equation (6) can be represented as

$$\iiint_W (\bar{l}_k \nabla I^k(\bar{r}) + \alpha(\bar{r}) I^k(\bar{r})) \cdot \psi_i(\bar{r}) \, dW = \iiint_W S^k(\bar{r}) \psi_i(\bar{r}) \, dW \quad (10)$$

for every $i = 1, \ldots, N_p$. According to equation (9), system of linear equations is received as

$$\bar{M}^k \cdot \bar{I}^k = \bar{Y}^k$$

where

$$M_{i,j}^k = \sum_{m=1}^{N_e} \iiint_{W_m} (\bar{l}_k \nabla \psi_j(\bar{r}) + \alpha(\bar{r}) \psi_j(\bar{r})) \cdot \psi_i(\bar{r}) \, dw$$

$$Y_i^k = \sum_{m=1}^{N_e} \iiint_{W_m} S^k(\bar{r}) \psi_i \, dw$$

$$\left(W = \sum_{m=1}^{N_e} W_m \quad W_m = m\text{th element} \right). \quad (11)$$

Boundary conditions are considered before solving the system (11). If the ith point is a boundary node and $(\bar{l}_k \cdot \bar{n}) < 0$, then I_i^k is computed by the formula (2). Then it is supposed that $M_{ij}^k = 0$ for every $J = 1, \ldots, N_p$, and $M_{ii}^k = 1$ and $Y_i^k = I_i^k$.

After this procedure the system (11) is solved by any known method (for example, it may be a Gaussian method) and radiative intensities along kth direction are found for all nodes I. After calculations for every selected directions the integral terms in equations (1) and (2) are calculated by the well-known quadratic Gaussian formula. For example:

$$Q_p^i \cong \sum_{m=1}^{N_d} A_m \cdot I_i^m \cdot \vartheta(\bar{l}_m, \bar{n}_i)$$

$$S_i^k \cong \sum_{m=1}^{N_d} A_m \cdot I_i^m \cdot p(\bar{r}_i, \bar{l}_k, \bar{l}_m) \qquad (12)$$

where A_m are weights of the Gaussian formula [12], albedo for scatter $p(\bar{r}_i, \bar{l}_k, \bar{l}_m)$ is determined according to equation (6) and $\vartheta(\bar{l}_m, \bar{n}_i)$ is determined by

$$\vartheta(\bar{l}, \bar{n}) = \begin{cases} \bar{l} \cdot \bar{n}, & \bar{l} \cdot \bar{n} \geqslant 0 \\ 0, & \bar{l} \cdot \bar{n} < 0. \end{cases} \qquad (13)$$

Equations (1) shows that the source's function, $S^k(\bar{r})$, and boundary conditions (2) depend on the radiative intensities. So it is necessary to organize an iterative process with successively more accurate definitions of radiation intensities. Thus, the proposed algorithm has the following structure.

(1) Values of radiation intensities are taken to be equal to zero or determined from some approximation solution which is faster. In the last case it should be noted that for successful solution the approximate values of radiation intensities must be less than that obtained from the solution problem (1, 2).

(2) Source's function, $S^k(\bar{r})$, and radiant flux density, $Q_p(\bar{r})$, are determined according to equations (8 and 9).

(3) Using the formula (11), matrix $\bar{\mathbf{M}}^k$ and vector $\bar{\mathbf{Y}}^k$ are estimated, and taking into account the boundary conditions the radiative intensity, $\bar{I}^k$, is calculated for every selected direction, $k = 1, \ldots, N_d$. At the same time the relative error is calculated in matching two successive iterative approximations (s and $s+1$) of radiation intensities

$$\delta = \max_{i,k} |1 - I_i^{k,s} / I_i^{k,s+1}|$$

(4) The validity of inequality $\delta \leqslant \delta_0$, where δ_0 is the given maximum relative error, is verified. If the condition is violated, then the calculation is repeated, beginning from item 2.

One iteration requires, approximately, 15 s of computing time on an AT/286 computer for 300 elements and 50 directions. Numerical experiments show that a relative accuracy of 0.001 can be achieved at 3–8 iterations at $Sc < 0.9$. The iteration number depend on the optical properties of medium and boundary surfaces.

The series of numerical experiments have been made for the appraisal of the proposed method accuracy. Comparison with results obtained by other authors was confirmed with its high efficiency and reliability for the calculation of radiative transfer characteristics in the selective absorbing, emitting and scattering media of complex geometry [8].

3. RESULTS

3.1. *Influence of the medium's optical properties*

Hereafter, the optical density of the medium (τ), albedo for scatter (Sc), the reduced density of outgoing radiant flux (q) and the reduced radiant intensity (i) are defined as

$$\tau = \chi_m \cdot L_o \quad Sc = \sigma/(\chi + \sigma)$$

$$q = Q_p/\pi \cdot B_2 \quad i = I/B_2$$

where χ_m is the average absorption coefficient, L_o is the average size of domain, $B_2 = B(T_{max})$, $B_1 = B(T_{min})$. The reduced temperature is defined as $\Theta = (T - T_{min})/(T_{max} - T_{min})$.

Investigation of the influence of medium optical properties on the radiative transfer characteristics is worthwhile carrying out on the model problems of a flat layer. This is important for the exception of the medium geometric form influence. Some results of the above investigation are reduced and illustrated below. The results meet the following conditions:

(1) A flat layer of absorbing, emitting and scattering medium is being considered, θ is a direction of ray propagation (Fig. 1).

(2) The results correspond to the following temperature distribution $\Theta(x)$ (Fig. 1, $T_{max} = 2000$ K and $T_{min} = 1000$ K).

(3) The spectral radiation is considered to be of a wavelength equal to 3 μm.

(4) Distributions of χ and σ are homogenous.

It is worthwhile accepting some other parameters for investigation of the dependence on radiative transfer characteristics from the optical density of medium. That is why we considered a flat layer with transparent boundaries [condition 2.3, $I_o(\bar{l}) = 0$]. The analysis of numerical investigation results allows one to detect the following special features of the influence of the optical density of media on the characteristics of radiative transfer:

(1) When $\Theta(x) = \text{const}$ (Fig. 1, curve 4) the outgoing radiant flux density is increasing and $q(\tau) \to 1$ as $\tau \to \infty$ (Fig. 2, curve 4, $Sc = 0$).

(2) If the medium is nonhomogeneous [$\Theta(x) \neq \text{const}$], then $q(\tau)$ has its pronounced maximum at a certain value of the optical density τ_o (Fig. 2, curves 1–3, numbers of curves correspond to numbers of the temperature distributions);

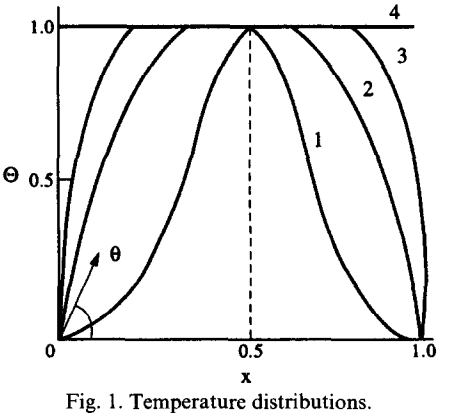

Fig. 1. Temperature distributions.

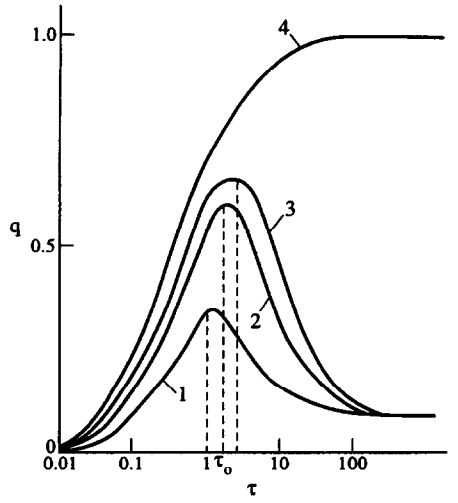

Fig. 2. Reduced density of outgoing radiative flux as a function of the optical density of medium.

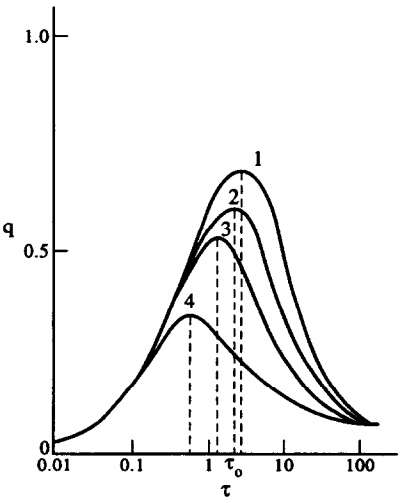

Fig. 4. Influence of scattering on the reduced density of outgoing radiative flux: (1) $Sc = 0$; (2) $Sc = 0.3$; (3) $Sc = 0.6$; (4) $Sc = 0.9$.

$q(0) = I_0/B_2$ and $q(\tau) = B_1/B_2$ as $\tau \to \infty$. Hereafter, this value of the optical density τ_0 will be referred to as a critical optical density. In the typical temperature range (1000–2000 K) for furnaces, the critical optical density does not practically depend on the wavelength and its value may be approximated as

$$\tau_0 \approx 1/^4\sqrt{1-s}, \quad \text{where} \quad s = \int_W \Theta(\bar{r})\,\mathrm{d}W \Big/ \int_W \mathrm{d}W.$$

(3) Outgoing radiant intensities $I(r, \bar{l})$ also have maximums, but in this case the critical optical density is a function of propagation direction (Fig. 3, temperature distribution—3).

The investigation of the influence of scattering processes on the radiative parameters has been carried out under the same conditions as for the influence of the optical density. Numerical experiments have shown that scattering decreases the outgoing radiant flux density q (Fig. 4, temperature distribution—3). However, it should be noted that the outgoing radiant intensity can increase depending on absorbing optical thickness of medium and single-scattering albedo (Figs. 5 and 6). The angular distribution of radiant intensity is illustrated by Fig. 6. This picture confirms the mentioned result on the influence of Sc and τ on the radiant intensities, so for a flat layer the optical thickness along the direction θ is defined by $\tau(\theta) = \tau/\cos\theta$. This result is very important for the definition of the selective component absorbing coefficient of the selectivity absorbing, emitting and scattering media in the finite spectral range and for the diagnostics of such media. Really, the effect described above occurs along the contour of the absorbing line and changes the transmissivity of the medium. Thus,

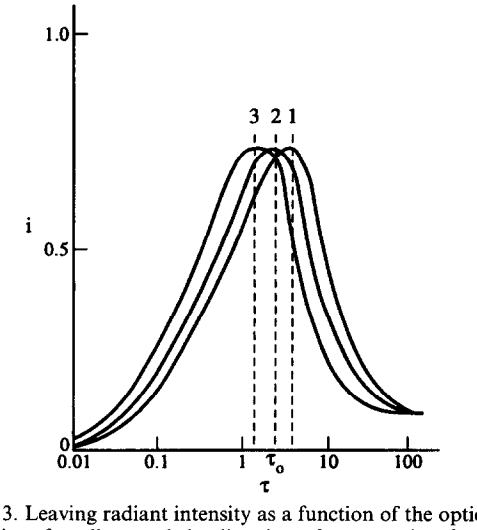

Fig. 3. Leaving radiant intensity as a function of the optical density of medium and the direction of propagation θ: (1) $\theta = 0$; (2) $3\pi/8$; (3) $\pi/4$.

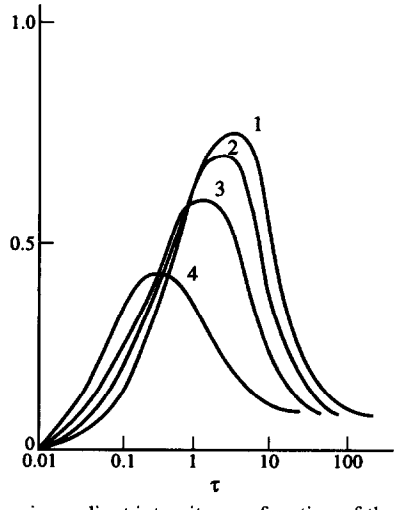

Fig. 5. Leaving radiant intensity as a function of the optical density of medium and the share of scattering processes: (1) $Sc = 0$; (2) 0.3; (3) 0.6; (4) 0.9.

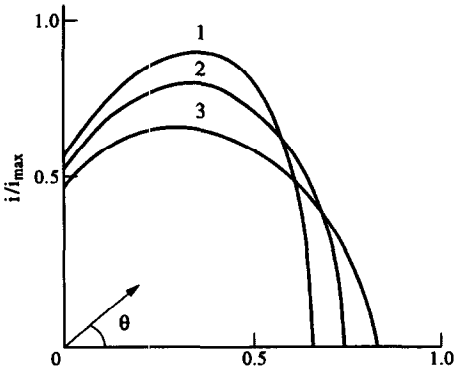

Fig. 6. The angular distribution of the leaving radiant intensity ($\tau = 0.5$): (1) $Sc = 0$; (2) $Sc = 0.3$; (3) $Sc = 0.6$.

the 'fine' line structure for a more correct determination of selective properties of medium should be taken into account. However, this process is complex and requires a long computation time. That is why it is worthwhile carrying out additional investigations to work out the averaging method for obtaining the average over the finite spectral range absorbing coefficient, as a function of the 'fine' line structure, medium thickness and scattering coefficient. At present we are investigating this problem.

The influence of boundary emissivity on the radiant transfer characteristics was also investigated for a flat layer for the diffuse-emitting boundary surface (condition 2.1). Numerical results show the outgoing radiant flux and the outgoing radiant intensity decreasing as a boundary emissivity ε is increasing (Fig. 7). However, net radiant flux $Q_n = \varepsilon \cdot (Q_p - \pi \cdot B(T_w))$ is increasing (Fig. 7).

3.2. *Influence of geometric form*

At this point, we study the influence of geometric form of domain on distribution of density of radiation

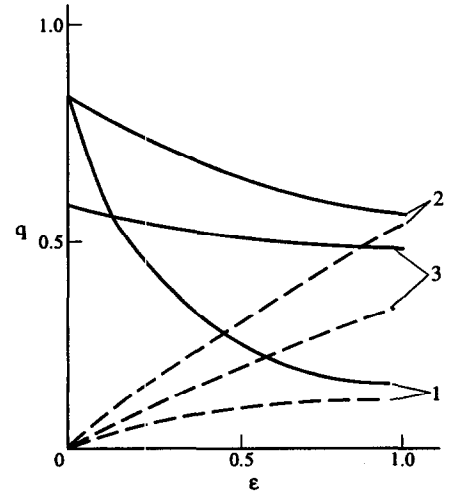

Fig. 7. Influence of boundary emissivity on the outgoing (——) and net (– – –) radiant flux density: (1) $\tau = 0.1$; (2) $\tau = 1$; (3) $\tau = 10$.

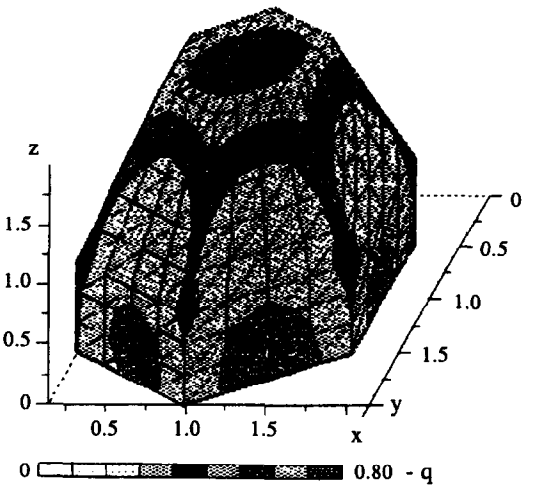

Fig. 8. Distribution of outgoing radiant flux on the boundary surfaces of emitting and absorbing medium.

fluxes (Q_p), falling on medium boundary surface, with homogeneous and constant values of medium's optical characteristics. The numerical investigation shows that nonhomogeneity of radiant fluxes distribution may achieve a substantial value. It is affirmed by Fig. 8 where the typical distribution of outgoing radiant fluxes is shown. The results have been received under the following conditions $\chi = 1.0$ m^{-1}; $\sigma = 0.0$ m^{-1}; the medium has a homogenous temperature distribution; the domain bottom is the specular surface and all other boundaries are the transparent surfaces (boundary condition 2.3), incident radiation is absent. Taking into account the complication of analysis of the 3-D distributions we will show the basic regularities of influence of geometric form on the radiative transfer characteristics for 2-D cases.

Hereafter, if another is not indicated the optical density of the medium is set equal to 1, the albedo for scatter (Sc) is set equal to 0, the emissivity of boundary surface $\varepsilon = 0.8$, the medium's temperature $T = 1300$ K, and the boundary temperature $T_w = 1100$ K.

The numerical investigation shows that the density of the radiative flux incident on the boundary surface depends on the distance between the given boundary portion and the center of the hot medium 's zone. The density of radiative flux (Q_p), is smooth function of the distance for smooth boundary.

At first, we consider the case in which the domain is a regular polygon. Under the above-mentioned conditions, the maximal value of the falling on the boundary surface radiant flux is on the middle of each side. The Q_p value decreases towards the domain corners. The typical flux distribution near the corner point of the right polygon is shown in Fig. 9. This picture illustrates the influence of the domain's geometry on the maximal 'reduced difference' which is determined as

$$\Delta Q = (Q_{max} - Q_{min})/Q_{max}. \qquad (14)$$

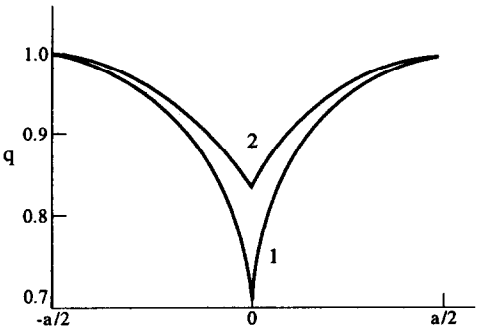

Fig. 9. Distribution of the density of reduced outgoing flux along the boundary of right triangular (1) and square (2) domains.

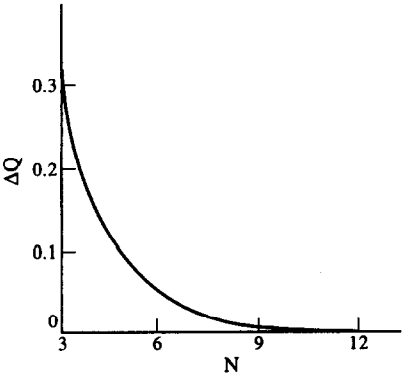

Fig. 10. The 'maximal reduced difference' of values of the outgoing radiant flux density along the boundary as a function of side's number of the regular polygon.

Increasing the side's number (N) of the regular polygon leads to the rapid decreasing of the ΔQ value. The distribution of Q_p along the boundary surface is practically homogenous at $N > 12$ (Fig. 10).

If the domain form differs from regular polygon, the value density of the radiant flux coming to a corner point from various sides may be different (Fig. 11)

$$\lim_{x \to P} Q_p(x) \neq \lim_{y \to P} Q_p(y).$$

This situation becomes clearer if we consider the angular distribution of the outgoing radiant intensity in

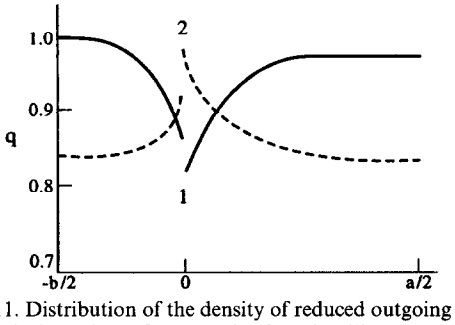

Fig. 11. Distribution of the density of reduced outgoing flux along the boundary of rectangular domain: (1) $T_W < T_b$; (2) $T_W > T_b$.

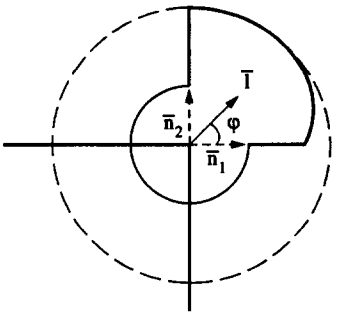

Fig. 12. The angular distribution of the radiant intensity at the corner point of rectangular domain.

the corner point (Fig. 12). The dotted line corresponds to the maximal value of the radiant intensity in the point. The analysis of these results shows that the value of 'reduced discontinuity' of outgoing radiant fluxes at the corner point.

$$\delta Q = \left| \lim_{x \to P} Q_p(x) - \lim_{y \to P} Q_p(y) \right| \Big/ Q_{p,\max} \qquad (15)$$

is not equal to zero if the bisector of the corresponding corner is not the symmetry axis of the domain, otherwise $\delta Q = 0$. This is confirmed by Fig. 13, where the distribution of the outgoing radiant flux on the boundary surfaces of a polygon with five sides is shown ($AB = DC = ED = a, BC = AE = 0.5a$). It should be noted that the same situation takes place when the symmetry of the optical characteristics of the medium and the boundary is broken. For example, if the square sides have a different temperature, then δQ is not equal to zero in the corner point.

Here, we analyze the dependence of ΔQ and δQ on the emissivity of the boundary surface, optical density of medium, profile of temperature and albedo for scatter. This study is carried out by the example of rectangle domain with sides a and b ($a = 2b$), when every other parameter of the medium is as described above.

The numerical analysis shows the ΔQ and δQ values' dependence of the relative difference between the boundary radiation and 'own' medium radiation. Here, 'own' medium radiation is the resulting radiation $J_0 + \partial J$, where J_0 is the intensity of the boundary radiation and δJ is its part absorbed or intensified by the medium. For example, the increasing of the boundary surface emissivity causes the increase in ΔQ and δQ, so, as with increasing ε 'own' boundary radiation $\varepsilon \cdot B(T_w)$ grows and it leads to further increasing of the nonhomogeneity of the radiant flux distribution on the boundary (Fig. 14).

The influence of the relative difference between the temperature of the boundary and the medium ($\delta T = (T_b - T_w)/T_b$) is illustrated in Fig. 15. The ΔQ and δQ dependence on δT has a linear character under the above-mentioned conditions. The increasing of leads to the growing of the nonhomogeneity of the outgoing radiant flux distribution on the boundary

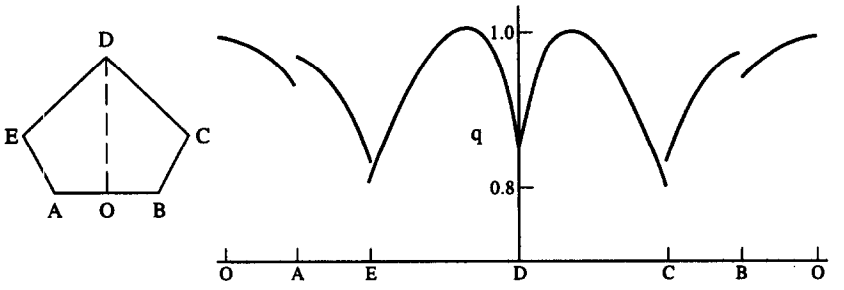

Fig. 13. Distribution of the radiative flux density along the boundaries of five-sides polygon.

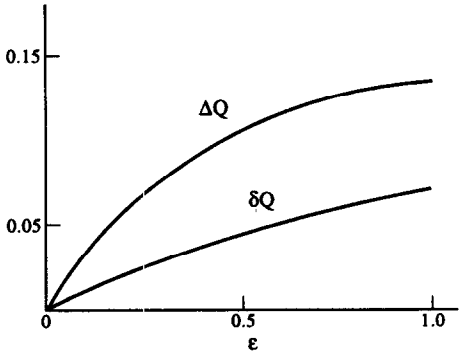

Fig. 14. Influence of wavelength (a) and boundary emissivity (b) on the values of ΔQ and δQ.

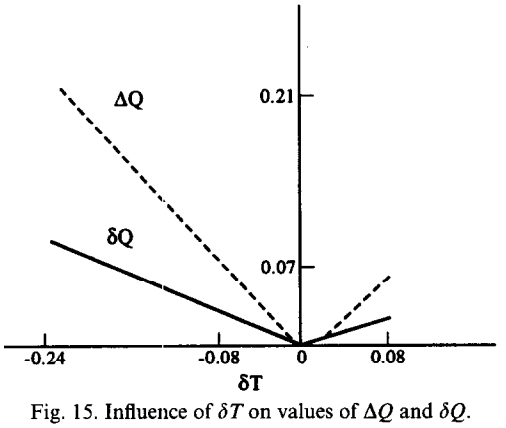

Fig. 15. Influence of δT on values of ΔQ and δQ.

surface. It is connected with the increasing of the relative difference between 'own' radiation of the boundary and the medium. Changing the sign of δT leads to the qualitative changing of the distribution of Q_p (Fig. 11, curve 2). As $\delta T < 0$ the Q_p value increases from the side middle to the corner point and the Q_p value increases from the corner point to the side middle, so the optical way of the incoming ray from the nearest boundary is shorter and the 'own' radiation of the boundary effects more actively.

It is of interest to consider the influence of the optical density of the medium on the distribution of the radiant flux falling on its boundary. The medium does not practically take part in the process of radiative transfer when $\tau \leqslant 0.01$. As the temperature of the boundary is homogeneous, so the distribution of the outgoing radiant flux on the boundary is homogeneous too. The 'own' radiation of the medium grows with increasing τ and it effects more actively on the radiative transfer. The nonhomogeneity of the radiant flux distribution increases too. The value of the maximal difference of the radiant flux density ΔQ has its pronounced extremum at the certain value of the optical density of nonhomogeneous medium (Fig. 16). The decreasing of ΔQ is observed as further increasing τ. This Δ behavior is connected with the nonhomogeneity of the medium temperature. More cold layers of the medium near the boundary begin to weaken the outgoing radiant fluxes and to lead to its more homogeneous distributions along the boundary. If the temperature distribution is homogeneous then the ΔQ value has not its pronounced extremum (Fig. 16, dotted line).

As $\tau \to 0$ and $\tau \to \infty$, the δQ value is equal to zero, the $\delta Q(\tau)$ dependence has the extremum (Fig. 16) for homogeneous and nonhomogeneous medium. As $\tau \to \infty$, one can obtain the formula to define the reduced incident radiant flux at the corner point of rectangular domain:

$$q = \frac{1}{1+\varepsilon}\left(1+\varepsilon\cdot\frac{B(T_w)}{B(T_b)}\right). \tag{16}$$

The influence of the albedo for scatter on the ΔQ and δQ is illustrated in Figs. 17 and 18. The increasing of the scattering leads to growing the maximal difference, ΔQ, and decreasing the corner point dis-

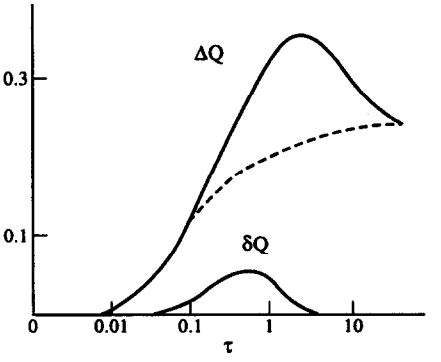

Fig. 16. Values of ΔQ and δQ as a function of the optical density of homogeneous (– – –) and nonhomogeneous (——) medium.

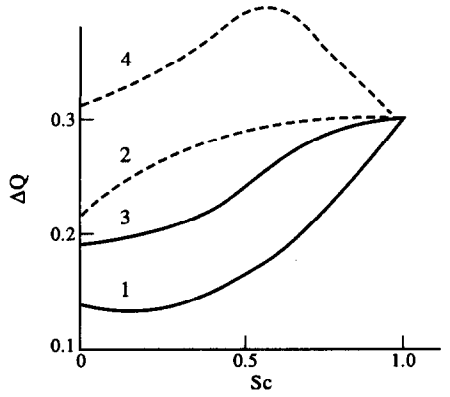

Fig. 17. Influence of Sc on the values of δQ for homogeneous (1,2) and nonhomogeneous (3,4) medium: ——$\tau = 0.5$; -- -- $\tau = 3.0$.

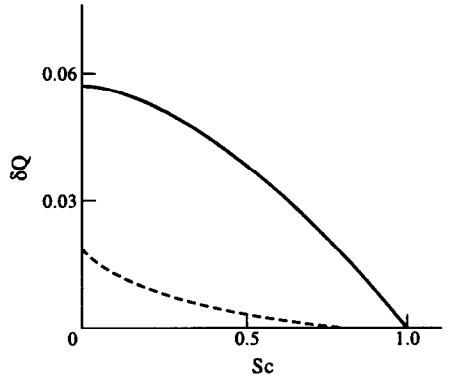

Fig. 18. Influence of Sc on the value of δQ.

continuity δQ (Fig. 18). If the medium is nonhomogeneous the ΔQ value may have its pronounced extremum at certain values of optical density and albedo for scatter of the medium.

4. CONCLUSION

An effective numerical solving algorithm of the integro-differential radiative transport equation has been proposed. The described method allows one to calculate the radiative intensities and fluxes in an absorbing, emitting and scattering medium of complex 3-D geometry. The numerical investigation of the influence of the medium's optical properties and boundary geometrical form on the radiation propagation in the above-mentioned media. The received results show possibilities of radiative heat transfer intensification by the control of the optical properties of the heat-transfer agent and boundary surfaces. The carried out investigation has shown that the form of domain filled with an absorbing, scattering and emitting medium essentially effects on the radiant flux distribution along its boundary surface. One may obtain more homogeneous flux distribution or other concentrate fluxes on some boundary part by the directive changing of the domain form. While designing the furnace chamber, one should take into account the influence features of the medium form on the radiative transfer characteristics.

REFERENCES

1. Siegel, R. and Howell, J. R., *Thermal Radiation Heat Transfer*, 3rd edn. Hemisphere, Washington D.C., pp. 795–804.
2. Hottel, N. C., Sarofim, A. F., *Radiative Transfer*. McGraw-Hill, New York, 1967, 512 p.
3. Menguc, M. and Viskanta, R., Radiative transfer in three-dimensional rectangular enclosures. *JQSRT*, 1985, **35,** 533–549.
4. Maruyama, S. and Aihara, T., Radiative heat transfer of arbitrary 3-D participating media and surfaces with non-participating media by a generalized numerical method REM. *Proceedings of the First International Symposium on Radiation Transfer*, Kusadasi, Turkey, 1995, pp. 153–167.
5. Adzerikho, K. S., Nogotov, E. F. and Trofimov, V. P., *Radiative Heat Transfer in Two-Phase Media*. CRC Press, Boca Raton, 1993, 160 p.
6. Fiveland, W. A., Discrete-ordinate solutions of the radiative transport equation for rectangular enclosures. *Journal of Heat Transfer*, 1984, **106,** 699–706.
7. Truelove, J. S., Three-dimensional radiation in absorbing–emitting–scattering media using the discrete-ordinates approximation. *JQSRT*, 1988, **39**(1), 27–31.
8. German, M. L., The influence of the optical properties of the two-phase medium and its boundary surfaces on the radiative heat transfer in the furnaces (in Russian). Ph.D. thesis, Heat and Mass Transfer Institute, Minsk, Belarus, 1993, 131 p.
9. Sobolev, V. V., *Radiative Energy Transfer in Atmospheres of Stars and Planets*. GITL, Moscow, 1956.
10. Adzerikho, K. S. and Nekrasov, V. P., Influence of anisotropic scattering on the luminescence of two-phase-media. *Journal of Engineering Physics and Thermophysics*, 1978, **34,** 894–896.
11. Zienkiewicz, O. C., *The Finite Element Method in Engineering Science*. McGraw-Hill, London, 1971.
12. Lowan, A. N., Davids, N. and Levenson, A., Table of the zeros of the legendre polynomials of order 1–16 and the weight coefficients for Gauss mechanical quadrature formula. *Bulletin of the American Mathematical Society*, 1942, **48,** 739–742.